Scientific Reports

https://doi.org/10.1038/s41598-026-42684-9

Article in Press

Advanced alginate- nutriosomes for enhanced oral delivery of fermented Echium amoenum polyphenols

Received: 19 October 2025

Accepted: 26 February 2026

Published online: 08 March 2026

Cite this article as: Khosroshahi E.D., Rached R.A., Serpe A. *et al.* Advanced alginate- nutriosomes for enhanced oral delivery of fermented Echium amoenum polyphenols. *Sci Rep* (2026). https://doi.org/10.1038/s41598-026-42684-9

Ehsan Divan Khosroshahi, Rita Abi Rached, Angela Serpe, Mona Ghaslani, Zeinab E. Mousavi, Maryam Salami, Maria Manconi, Maria Letizia Manca, Olga Osmolowskaya, Elvira Escribano-Ferrer & Seyed Hadi Razavi

Advanced alginate- nutriosomes for enhanced oral delivery of fermented Echium amoenum polyphenols

Ehsan Divan Khosroshahi [a], Rita Abi Rached [b], Angela Serpe[c], Mona Ghaslani[c], Zeinab E. Mousavi[d], Maryam Salami [a,e], Maria Manconi [b], Maria Letizia Manca [b,*], Olga Osmolowskaya [f], Elvira Escribano-Ferrer[g], Seyed Hadi Razavi [a,e*]

[a] Bioprocess Engineering Laboratory (BPEL), Department of Food Science and Engineering, Faculty of Agricultural Engineering and Technology, University of Tehran, Karaj 31587-77871, Iran

[b] Department of Life and Environmental Sciences, University of Cagliari, University Campus, Pad. A, S.P. Monserrato-Sestu Km 0.700, 09042 Monserrato, CA, Italy

[c] Department of Civil and Environmental Engineering and Architecture (DICAAR), University of Cagliari, Piazza d'Armi, 09123 Cagliari, Italy

[d] Bioprocessing and Biodetection Laboratory, Department of Food Science and Engineering, Campus of Agriculture and Natural Resources, University of Tehran, Karaj, Iran

[e] Functional Food Research Core, University of Tehran, Tehran, Iran

[f] Institute of Chemistry, Saint Petersburg State University, 7/9 Universitetskaya Nab., St. Petersburg, 199034, Russia

[g] Biopharmaceutics and Pharmacokinetics Unit, Institute for Nanoscience and Nanotechnology, University of Barcelona, Barcelona, Spain; eescribano@ub.edu

[*] Corresponding authors.

E-mail address: mlmanca@unica.it (M.L.Manca), srazavi@ut.ac.ir (S.H. Razavi).

Abstract

Echium amoenum, a highly valued medicinal plant in Iran, is rich in polyphenols. Microbial fermentation can improve the bioavailability of its phenolic compounds, which are otherwise limited (5-10%), by releasing them from the plant cell wall. Moreover, incorporating these bioactive compounds in phospholipid vesicles can further maximize their biological efficacy. This study developed a combined approach using lactic acid fermentation with *Lactiplantibacillus plantarum* and phospholipid-based nanocarriers to optimize the delivery of *E. amoenum* extract. Fermented extract (50 mg/mL) was successfully incorporated into liposomes, nutriosomes, and advanced alginate-nutriosomes, as confirmed by cryo-TEM and FTIR analyses. All vesicles were nanosized (105–124 nm), negatively charged (~ –56 mV), and homogeneously dispersed (PDI ≤ 0.19) with high loading efficiencies (> 90%). They remained stable under simulated saliva, gastric, and intestinal conditions and exhibited controlled release. *In vitro* assays demonstrated biocompatibility and protective effects on stressed Caco-2 cells. Overall, alginate-nutriosomes represent a promising nanocarrier for oral administration of fermented *E. amoenum* extract.

Keywords: Medicinal plant extract; Polyphenols and Fermentation; Alginate; Nutriosomes; Oral delivery; Caco2 Cells Bioavailability.

1. Introduction

Since ancient times, plants have played a fundamental role in human health and nutrition, providing not only food and flavoring agents but also a vast array of therapeutic agents [1,2]. Among them, medicinal plants (MPs) have received considerable attention due to their broad spectrum of pharmacological activities, offering preventive and therapeutic benefits across numerous diseases [3,4]. The therapeutic effects of MPs are primarily attributed to their rich phytochemical content [3,4], and also the successful target tissue delivery, which highlights their bioavailability [5]. The biological efficacy of these bioactive compounds can be maximized through their incorporation into phospholipid vesicles [6].

MPs are one of the most important natural sources for drug discovery, both in traditional medicine and modern pharmacology [7]. The demand for MPs has consistently exceeded one million tons annually, primarily driven by growing interest in nutraceuticals, remedies, cosmetics, and other products derived from natural resources in Western countries. Statistical data indicate that approximately 45,000 plant species are currently recognized for medicinal use, representing an invaluable reservoir of bioactive compounds for novel therapeutic development [8]. Numerous MPs are rich in antioxidants, particularly polyphenols, which are crucial for neutralizing free radicals and ensuring human homeostasis. Their use is important in

preventing major health issues such as diabetes, skin disorders, Alzheimer's, Parkinson's, cancers, and oxidative damages [9].

Among various MPs, *Echium* species, belonging to the Boraginaceae family, have emerged as valuable medicinal resources. Distributed across diverse biogeographical regions, including the Macaronesian Islands, the Mediterranean Basin, and the Irano-Turanian region [10], *Echium* species are characterized by their distinctive purple or blue flowers [11]. Within the Iranian species, *E. amoenum* has been traditionally used for its medicinal properties, commonly prepared as decoctions for its tonic, soothing, and antitussive effects [10]. The dried petals of *E. amoenum* exhibit strong antioxidant, anti-inflammatory, anxiolytic, antiviral, and antidepressant properties [12], primarily attributed to their diverse phytochemical profile, including gallic acid, catechin, hydroxybenzoic acid, chlorogenic acid, caffeic acid, vanillic acid, epicatechin, ρ-coumaric acid, ferulic acid, rosmarinic acid, carotenoids and anthocyanins such as cyanidin-3-glucoside, cyanin chloride, cyanidin-3-rutinoside, and pelargonidin-3-glucoside [10]. To address the growing demand for natural molecules used in the treatment of various diseases, several studies have demonstrated that fermentation, an ancient, natural, and cost-effective process that now plays a key role in modern biotechnological approaches [13], can significantly enhance the release of conjugated phenolic compounds, improve the extraction of polyphenols and flavonoids, and stimulate the production of bioactive metabolites, including organic acids, proteins, amino acids, ceramides, enzymes, and antioxidants. As a result, fermentation not only increases the bioavailability of these compounds but may also enhance their biological activity while reducing potential cytotoxic effects [2,14–16]. However, clinical application of the fermented extract obtained from dried petals of E. amoenum is limited by low bioavailability, rapid metabolism, and instability of phenolic compounds in gastrointestinal conditions, which result in extensive degradation and insufficient absorption upon oral administration.

The biological efficacy of these bioactive compounds can be maximized incorporating them into phospholipid-based vesicular systems, which are well known as effective carriers to further enhance their stability, protection, and targeted delivery [6]. Phospholipid-based nanocarriers are considered highly advantageous for antioxidant compounds delivery due to their excellent biocompatibility, ability to improve solubility, and protection capacity from degradation [6,17]. More specifically, they possess a flexible and resilient bilayer structure that improves the bioavailability of encapsulated compounds, by facilitating both membrane fusion and cellular uptake. These nanocarriers, prepared via green, scalable, and reproducible methods using biocompatible and biodegradable materials, have demonstrated considerable promise across pharmaceutical, cosmetic, functional food, and nutraceutical research [17].

In this context, recent studies have demonstrated that the incorporation of Nutriose FM06®, a water-soluble, corn-derived branched dextrin with high fiber content, into phospholipid vesicles has led to the development of nutriosomes, a new class of highly effective vesicular nanocarriers particularly suitable for the delivery of plant-derived bioactive compounds or phytocomplexes to the intestinal tract [6,18–20]. It can act as structural component improving the stability of phospholipid bilayer and, at the same time, exert a functional role as prebiotic agent [21,22]. This compound is structured with dextrin linked by digestible α-1,6 glycosidic linkages, alongside non-digestible α-1,2 and α-1,3 glycosidic linkages. Due to its chemical structure, merely 10-15% of the fiber is absorbed in the stomach and small intestine, with the rest undergoing gradual fermentation in the colon, providing a prebiotic effect [6]. Despite the promising performance of Nutriosomes for oral delivery, previous studies have highlighted that Nutriose FM06 alone may not provide sufficient protection to natural compounds against the harsh conditions of the gastrointestinal tract. Enhancing Nutriosomes with an additional polymeric component can significantly improve the stability of sensitive bioactive molecules, prevent

their premature degradation, and enable a more controlled and sustained release once they reach the physiological environment. Such polymer-enriched Nutriosomes therefore represent an important advancement in the design of innovative carriers for the effective oral administration of natural compounds [22–26]. Among natural polymers, alginate, a water-soluble polysaccharide obtained from brown algae and some bacterial species, represents an excellent candidate for the delivery of fermented *E. amoenum* extract. Owing to its outstanding biocompatibility, biodegradability, and its well-documented ability to modulate drug release, alginate has been widely employed as an encapsulating material in advanced oral delivery systems [27]. Incorporating alginate into Nutriosomes may enhance their structural integrity and prevent aggregation, thereby improving shelf-life and dispersion. Moreover, alginate provides protective effects against harsh gastro-intestinal conditions by forming a gel barrier, which helps to sustain the release and bioavailability of encapsulated antioxidant and polyphenolic compounds. Previous studies have confirmed that alginate-based nanoparticles effectively enhance the chemical stability and controlled release of these bioactive compounds, making it a key ingredient for improving on one side the physicochemical features and on the other side the therapeutic efficacy [28,29]. Owing to their solubility in water, these substances have found extensive application in the entrapment of hydrophilic nutraceuticals, β-carotene, and antibiotic agents [30]. Moreover, the integration of alginate with various biopolymers, including polysaccharides and proteins, has been considered to enhance its efficacy as an encapsulation agent for water-soluble polyphenols [31].

Therefore, the present study aimed to design, optimize, and evaluate novel alginate-nutriosome-based nanocarriers for the oral delivery of polyphenol-rich fermented *E. amoenum* extract (FEAE), using an environmentally friendly preparation method that employs safe, naturally derived materials (phospholipids, Nutriose FM06®, and alginate). This dual strategy addresses a critical gap related to stability, bioavailability, and gastro-intestinal

degradation of *E. amoenum* extract, providing a promising approach for the development of effective antioxidant therapies. The *in vitro* characterization and efficacy of these innovative delivery systems were assessed to preliminarily explore their potential applications as advanced nutraceutical formulations.

2. Materials and Methods

2.1. Materials

Raw and fresh flowers of *E. amoenum* were provided from a local store in Alborz, Iran, shade-dried at room temperature (25 °C), finely ground with a high-speed electric grinder, and then sieved (60-mesh). Both harvesting and processing have been performed according to the IUCN Policy Statement on Research Involving Species at Risk of Extinction and the Convention on the Trade in Endangered Species of Wild Fauna and Flora. The resulting powder was refrigerated in a two-layer package (aluminum and polyethylene) until extraction. Soy phosphatidylcholine (Lipoid® S75, S75) was purchased from Lipoid GmbH (Ludwigshafen, Germany). Nutriose FM06® was kindly provided by Roquette (Lestrem Cedex, Beinheim France). Sodium alginate was purchased from Galeno (Potenza, Italy). Phosphate buffered saline (PBS, pH 7.0), 2,2- diphenyl-1-picrylhydrazyl (DPPH), and all other reagents of analytical grade were purchased from Sigma-Aldrich (Milan, Italy). Besides, cell medium, fetal bovine serum, penicillin and streptomycin and all other reagents for cell studies were obtained from Thermo Fisher Scientific Inc. (Waltham, MA, USA).

2.2. Starter microorganisms

Lyophilised *Lactiplantibacillus plantarum* (DSM 20179) was provided by the Bioprocess Engineering Laboratory (BPEL, University of Tehran, Iran) and revived twice using sterilized MRS (Man Rogosa and Sharpe) broth (Merck, Darmstadt, Germany) at 37 °C for 16 h. All stock cultures were stored at −

20 °C in MRS broth containing 40 % sterile glycerol. After two successive transitions in sterilized MRS broth, they were cultured in sterilized MRS broth at 37 °C for 24 h to achieve cell concentrations of approximately 9 log CFU/mL [32].

2.3. Preparation of polyphenol-rich fermented E. amoenum extract (FEAE)

Initially, 8 g of raw *E. amoenum* dry powder was mixed with 100 mL of distilled water and then subjected to sterilization for 15 min at 121 °C. Following sterilization, *L. plantarum* (DSM 20179) was inoculated (109 CFU), and then the mixture was incubated at 37°C for 24 h using a shaker incubator (Stuart Orbital Incubator S150) with 50 rpm. During the fermentation process, pH was measured at 4-hour intervals to monitor the bacterial growth and activity. After fermentation, the supernatant portion was separated using a benchtop refrigerated centrifuge at 6000 rpm for 15 minutes at 4°C, followed by filtration with Whatman filter paper. Then, the filtrates (FEAE) were lyophilized (Dena Vacuum Industry, Co., Ltd.) to obtain fine powder. The resulting powder was stored at -20°C for further analysis. Each treatment was performed in triplicate.

2.4. Quantitative determination of rosmarinic acid using ultra performance liquid chromatography coupled with photodiode array detection (UPLC-PDA)

Analyses were performed using Ultra Performance Liquid Chromatography (UPLC) equipped with a photodiode array (PDA) detector (Waters ACQUITY UPLC H-Class system, Milford, MA, USA). Separation was performed on an ACQUITY UPLC BEH C18 column (2.1 × 150 mm, 1.7 µm particle size) at 40 °C. The mobile phase consisted of solvent A (0.1% formic acid in water) and solvent B (0.1% formic acid in acetonitrile) with a gradient elution as follows: 97% A and 3% B at 0 min; 97% A and 3% B at 5 min; 90% A and 10% B at 10 min; 85% A and 15% B at 15 min; 80% A and 20% B at 20 min; 70% A and 30% B at 25 min; 60% A and 40% B at 30 min; 40% A and 60% B at 33 min; 10% A and 90% B at 35 min; 97% A and 3% B at 37 min; and 97% A and 3% B at 40 min, and returned to initial conditions for column equilibration.

The flow rate was set at 0.2 mL/min, and the injection volume was 2 µL. Detection was carried out at 313 nm, and rosmarinic acid was identified and quantified by comparing the retention time and UV spectrum with that of an external standard. The sample concentration was adjusted to 1 mg/mL before injection. Data collection and processing were conducted utilizing Waters Empower™ 3 software (Waters Corp., Milford, MA, USA). A calibration curve was constructed using standard solutions of rosmarinic acid in the concentration range of 0.5 to 0.005 mg/mL ($R^2 > 0.99$).

2.5. Total phenolic content (TPC) and antioxidant activity

The Folin-Ciocalteu colorimetric method using a UV spectrophotometer (Lambda 25, PerkinElmer, Waltham, MA, USA) was applied to determine the TPC of the FEAE as described by Castangia et al. [6]. A mixture of ethanolic extract solution (100 µL, 1 mg/mL) with Folin-Ciocalteu reagent (100 µL) and sodium carbonate solution (800 µL, 20% w/v) was prepared. Then, after 30 minutes of incubation in the dark at 25 °C, the absorbance was measured at 765 nm. Total phenolic content, expressed as mg gallic acid equivalents/g dry extract, was determined using a gallic acid calibration curve (0–0.100 mg/mL) and performed in triplicate.

To assess the antioxidant properties of the extract, its effectiveness in scavenging DPPH (2,2-diphenyl-1-picrylhydrazyl) radicals was measured. The ethanolic solution of the extract (20 µL, 1 mg/mL) was mixed with 1980 µL of DPPH (40 µg/mL in methanol) and allowed to incubate in the dark at room temperature for 30 min. Absorbance was then measured at 517 nm against a blank [33].

The calculation of antioxidant activity (AA) was performed using the following formula:

$$\text{AA } (\%) = \frac{X\,DPPH - X\,Sample}{X\,DPPH} \times 100$$

A calibration curve was obtained using trolox (6-hydroxy-2,5,7,8-tetramethylchroman-2-carboxylic acid) at different concentrations (0–0.010 mg/mL), which served as a reference. The antioxidant activity was quantified as mg of trolox equivalent/g of dry extract. All experiments were conducted in triplicate.

2.6. Vesicle preparation

Liposomes were prepared by dissolving Lipoid® S75 (120 mg/mL) and FEAE (50 mg/mL) in 1 mL of bi-distilled water in a glass vial. For the preparation of nutriosomes, Nutriose FM06® (120 mg/mL) was added to the lipid and extract mixture prior to hydration. The resulting aqueous dispersions were then sonicated using a Soniprep 150 ultrasonic disintegrator (MSE Crowley, London, UK) following three cycles (10 + 10 + 5), with each cycle consisting of 5 seconds of sonication followed by 2 seconds pause, at a probe amplitude of 13 µ, allowing the samples to cool between cycles.

For the preparation of alginate-nutriosomes, alginate solutions (0.1–1% w/v) were first prepared in bi-distilled water. Subsequently, 1 mL of each alginate solution was used to hydrate the lipid and extract mixture, followed by sonication for 10 cycles (5 s on, 2 s off) at a probe amplitude of 13 µ. After optimization, an alginate concentration of 0.8% w/v was selected for further analyses. Empty formulations (without the extract) were also prepared and used as controls for comparative purposes. The sample composition is reported in Table 1

Table 1. Composition of FEAE-loaded nanocarriers (Liposomes, nutriosomes, and alginate-nutriosomes)

	S75 (mg/mL)	**FEAE (mg/mL)**	**Nutriose (mg/mL)**	**Alginate solution (%)**

Liposomes	120	50	-	-
Nutriosomes	120	50	120	-
Alginate-nutriosomes	120	50	120	0.8

2.7. Characterization of vesicles

2.7.1. Formation and morphology

Formation and morphology of vesicles were investigated using cryogenic transmission electron microscopy (cryo-TEM) analysis. A 5 µL sample was placed on a grid Lacey carbon film (Electron Microscopy Science, Hatfield, PA, USA). The grid was mounted on an automatic plunge freezing apparatus (Vitrobot FEI, Eindhoven, The Netherlands) to control humidity and temperature, immersed in liquid ethane, fast cooled from outside by liquid nitrogen, avoiding the formation of ice crystals. A Tecnai F20 microscope (FEI, Eindhoven, The Netherlands) operating at 200 kV, equipped with a cryo-specimen holder Gatan 626 (Warrendale, PA, US) was utilized to perform the observations at approximately – 170 °C. Digital images were captured with an Eagle FEI camera, 4098 × 4098 pixels. Magnification was set between 20,000 –30,000× with a de-focus range of 2–3 µm.

2.7.2. Dynamic light scattering (DLS) analysis

The mean diameter and polydispersity index (PDI; a measure of the size distribution width) were assessed through DLS utilizing a Zetasizer Ultra (Malvern Instruments, Worcestershire, UK) [34]. The samples were subjected to backscattering by a helium-neon laser operating at a wavelength of 633 nm, measured at an angle of 173°, and maintained at a consistent temperature of 25 °C.

The Zetasizer Ultra was also applied to determine the surface charge of vesicles (zeta potential), measuring their electrophoretic mobility in dispersion by the mixed-mode measurement-phase analysis (M3-PALS). Each

sample was diluted with water (1:100) before analysis to ensure optical clarity and prevent laser beam attenuation and scattered light reduction.

2.7.3. Entrapment efficiency

The entrapment efficiency was determined by calculating the percentage of antioxidant activity in vesicle dispersions prior to and following their purification through dialysis, which removed the unentrapped extract. A volume of 1 mL of the vesicle dispersions was placed into a dialysis tube (Spectra/Por® membranes, 12–14 kDa MW cut-off, 3 nm pore size; Spectrum Laboratories Inc., DG Breda, The Netherlands) and kept at room temperature in water (1 L), with continuous stirring for 2 hours, during which the water was refreshed after the first hour. The antioxidant activity of the dispersions was assessed before and after dialysis using the DPPH colorimetric assay, as previously described.

2.8. Vesicle behavior at salivary and gastro-intestinal pHs

The simulant saliva solution was prepared by dissolving 2.38 g Na_2HPO_4, 0.19 g KH_2PO_4, and 8 g NaCl in 1 L of distilled water, with pH adjusted to 6.75 using phosphoric acid.

A pH 1.2 gastric fluid simulant was prepared per USP XXIV (US. Pharmacopeia XXIV, 2006) and (European Pharmacopeia X, 2020) guidelines, without enzymes, by dissolving 1.75 g NaCl in a solution composed of 94 mL distilled water and 6 mL 1 M HCl.

Neutral intestinal fluid simulant (pH 7.0) was prepared by dissolving 7.26 g Na_2HPO_4, 3.56 g NaH_2PO_4, and 17.54 g NaCl in distilled water to a final volume of 1 L.

The vesicles were subjected to a dilution of 1:500 using fluids, and the average diameter, PI, and zeta potential of the vesicles were measured after incubation in the medium at pH 6.75 for 10 min, at pH 1.2 for 2 h, and at pH 7 for 6 h at 37°C.

2.9. Fourier-transform infrared spectroscopy (FT-IR) analysis

An Avatar spectrometer (Thermo Nicolet, Waltham, MA, USA) was employed to assess both the empty formulated vesicles and those loaded with the FEAE. The samples underwent examination across the wavenumber spectrum of 4000 to 500 cm^{-1} in transmittance mode, with a resolution set at 4 cm^{-1}.

2.10. Release studies

To determine the amount of extract released from the vesicles, a dissolution tester with 6 stations (DT 720 Series—Erweka, distributed by EMME 3 SRL, Milan) was utilized, following USP requirements. Vesicle dispersions were placed into polycarbonate dialysis tubes (Spectra/Por membranes: 12–14 kDa MW cut-off, 3 nm pore size; Spectrum Laboratories Inc., NJ, USA), and positioned in the baskets of the dissolution tester, which contained 1 liter of release media. The setup was maintained under continuous stirring at 37 °C for a duration of 48 hours. The extract concentration in the dispersion was analyzed at intervals of 0.5, 1, 2, 4, 6, 8, 24, and 48 h by measuring antioxidant activity through the DPPH colorimetric assay [35].

2.11. Biocompatibility of vesicles

Caco-2 cells (Caco-2, ATCC HTB-37 collection, USA) were cultured as monolayers in 75-cm^2 flasks at 37 °C with 5% CO_2 and 100% humidity, using high-glucose Dulbecco's Modified Eagle Medium (DMEM) supplemented with 10% fetal bovine serum and 1% penicillin/streptomycin. The MTT (3-[4, 5-dimethylthiazol-2-yl]-3, 5 diphenyl tetrazolium bromide) assay was employed to determine cell viability [36]. In each well of a 96-well plate, 7.5×10^3 cells were seeded. Following a 24-h incubation period, 25 µl of each sample, which included FEAE either in aqueous dispersion or loaded into vesicles, was administered to the cells. The extracts had been previously diluted to achieve the target concentrations of 0.005, 0.05, 0.5, and 5 µg/mL. Upon completion of 48 h of incubation, MTT solution (final concentration of 0.5 mg/mL) was added to each well, then removed after 3 h and substituted with dimethyl

sulfoxide. Absorbance measurement of the solubilized dye was recorded at 570 nm with a microplate reader (Multiskan EX, Thermo Fisher Scientific Inc., Waltham, MA, USA). The viability of the treated cells was calculated as a percentage in relation to the untreated control cells, which were considered to have 100% viability [37].

2.12. Protective effect of vesicles against damage induced in cells by oxidative stress

Caco-2 cells were plated in 96-well plates at a density of 7.5 x 10^3 cells per well. After a 24-h incubation, the cells were subjected to stress via hydrogen peroxide (30% diluted to 1:40,000) while also being treated simultaneously with FEAE, either in aqueous dispersion or loaded vesicles, at a final biocompatible concentration of 5 µg/mL. Cells treated with hydrogen peroxide alone served as a negative control, while untreated cells (100% viability) served as a positive control. Following a 4-h incubation time, the cells were washed with phosphate-buffered saline (PBS) at pH 7.4, and their viability was evaluated through the MTT assay, as described above.

2.13. Statistical analysis of data

Results are presented as the mean ± standard deviation. Multiple group comparisons were performed using ANOVA, and the Tukey's test and Student's t-test were performed to substantiate differences between groups using Excel Statistics for Windows. The differences were considered statistically significant for $p < 0.05$.

3. Results and Discussion

3.1. Quantification of rosmarinic acid

The content of rosmarinic acid in the FEAE, which has been previously detected as the primary component of *E. amoenum* flowers [9,10], was determined by means of UPLC analyses. In the UPLC–PDA chromatogram of

the extract, a distinct peak was observed at a retention time of 12.27 minutes, corresponding to rosmarinic acid, as confirmed by the standard solution, Figure 1. The peak area was determined using Empower 3 software. Based on the sample peak area and the regression equation of the calibration curve, the concentration of rosmarinic acid in the fermented extract was calculated to be 14.053 µg/mL. Previous studies have proved that microbiological fermentation leverages microorganisms to modify and enhance the bioactive potential of plants. By breaking down plant cell walls and promoting hydrolysis, fermentation increases the extract content of polyphenols, flavonoids, organic acids, proteins, ceramides, amino acids, biological enzymes, and antioxidants in raw plant resources [2,14]. In particular, LAB fermentation demonstrably improves the bioactive potential of raw plants [2,33,38]. As confirmation of the better performances of fermentation, in a previous study, the concentration of rosmarinic acid in *E. amoenum* extracts varied between 2.02 and 2.4 mg/100 mg extract depending on the conventional extraction method selected [9]. Moreover, in a separate investigation, the use of ultrasonic-assisted ethanolic extraction resulted in a rosmarinic acid concentration of 2.657 mg/100 mg extract [10].

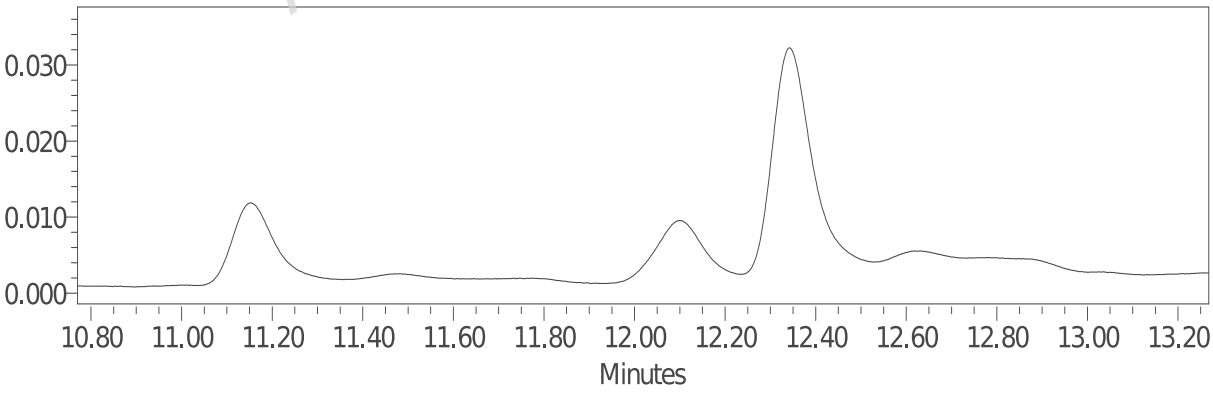

Figure 1. UPLC-PDA chromatograms of FEAE.

3.2. Total Phenolic Content (TPC) and antioxidant activity

The FEAE exhibited a high TPC of 289.56 mg GAE/g of dry extract and an antioxidant activity of 220.3 mg TE/g dry extract. These findings corroborate the research conducted by Asghari et al. (2019), which indicated that the TPC in Iranian *E. amoenum* ranged from 90.2 to 296.2 mg GAE/g extract based on different extraction methods. They also reported the IC50 value of 22.8 µg/mL as the highest DPPH radical scavenging activity [9]. Besides, Firoznezhad et al. (2023) reported values of 104 mg GAE/g extract and 21 mg GAE/g extract for the TPC and DPPH radical scavenging activity of ultrasonic-assisted ethanolic extract of *E. amoenum*, respectively.

Consistent with prior findings, LAB fermentation significantly enhances the antioxidant activity of plant extracts [2,16,39]. This improvement is correlated with elevated phenolic content, primarily resulting from the activity of microbial enzymes to transform bound and conjugated polyphenols into their free forms [2,39,40]. During the fermentation process, LAB produces lactic acid and CO_2, resulting in a decrease in pH level. This pH reduction is a key indicator of successful fermentation [41], with the pH value reflecting bacterial activity and growth [33]. In this study, the pH decreased from an initial value of 6.31 in the raw *E. amoenum* sample to 4.88 after 24 hours of fermentation with *L. plantarum*. Furthermore, LAB consume nutrients from the substrate to promote their growth, while also enabling the bioconversion of compounds through structural alterations, thereby enhancing the levels of metabolites with significant antioxidant properties [42]. More specifically, microbial enzymes such as cellulases and pectinases decompose cell walls, which promotes the release of active ingredients. They also convert glycosides, phenolic acids, and proteins into bioactive metabolites via glycosyl hydrolases, phenolic acid decarboxylases, and reductases. Moreover, fermentation may promote the biosynthesis of additional antioxidant enzymes such as superoxide dismutase and catalase,

further contributing to the enhanced antioxidant properties observed in plants [2,43]. Consequently, this process leads to an increased hydroxyl groups, which are considered key contributors to the observed beneficial activity [39]. Recent findings indicate that lactic acid fermentation-assisted extraction improves the recovery of antioxidants from fig leaves compared to single-solvent extraction methods applied to non-fermented samples [44]. Fessard et al. (2017) reported that lactic acid fermentation of tea extracts resulted in alterations in phenolic compounds, leading to elevated antioxidant activity [45]. In another research, Eweys et al. (2022) reported that the increased antioxidant properties observed in *Cinnamomum cassia* fermented with *L. plantarum* could be attributed to an elevation in specific phenolic and flavonoid compounds [46]. Furthermore, LAB fermentation of rambutan juice using *L. plantarum* and *Limosilactobacillus fermentum* improved both antioxidant activity and flavor complexity [47]. In another recent study, fermenting ginger using *Bifidobacterium adolescentis* and *Monascus purpureus* significantly increased gingerol, total flavonoids, and polyphenol levels, leading to improved antioxidant activity [48].

3.2. Physicochemical characterization of vesicles

At a high concentration of 50 mg/mL, FEAE was successfully incorporated into liposomes, nutriosomes, and alginate-nutriosomes via direct sonication, an environmentally friendly technique suitable for food additive applications, avoiding the use of pollutant organic solvents [6]. A preformulation study was conducted to identify the most promising vesicular systems in terms of stability, size, and loading capacity. Different types and concentrations of phospholipids and biopolymers were screened, and their ability to incorporate increasing amounts of FEAE was systematically evaluated. Among the tested phospholipids, Lipoid® S75 (120 mg/mL) was selected because it consistently produced vesicles with optimal physicochemical properties. A loading concentration of 50 mg/mL FEAE was identified as the

most suitable, ensuring efficient entrapment without compromising vesicle integrity.

Nutriose FM06 was incorporated at 120 mg/mL to improve structural stability and prevent aggregation; lower concentrations yielded unstable vesicles, whereas higher concentrations resulted in increased particle size and reduced homogeneity. Regarding alginate, different concentrations (from 0.1% to 1% w/v) were tested. For each concentration, particle size, polydispersity index, zeta potential, and vesicle stability were thoroughly evaluated in simulated gastro-intestinal conditions, including saliva, gastric, and intestinal fluids, over different time intervals. Based on these investigations, only 0.8% (w/v) provided adequate stabilization of the final vesicles without negatively affecting their morphology or dispersion quality.

The resulting formulations were characterized for mean diameter, polydispersity index, and surface charge, and the outcomes were compared across the different component combinations, using empty vesicles as the reference system (Table 2).

Cryo-TEM analysis confirmed vesicle formation (Figure 2). As can be observed, liposomes were mostly unilamellar with a few multilamellar vesicles (Figure 2A). The nutriosomes and alginate-nutriosomes were spherical in shape, and both uni- and multi-lamellar and multicompartment structures were observed (Figure 2B and 2C).

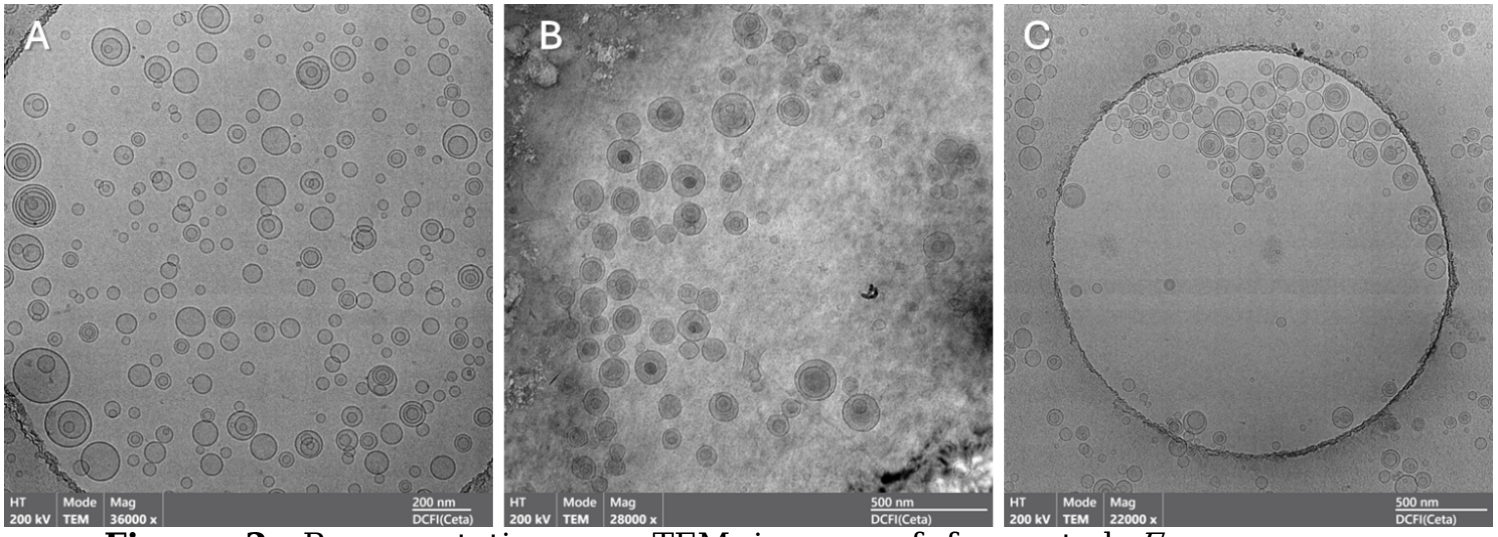

Figure 2. Representative cryo-TEM images of fermented *E. amoenum* extract-loaded liposomes (A), nutriosomes (B), and alginate-nutriosomes (C).

To evaluate the impact of components and payloads on vesicle assembly and structural characteristics, the diameter, PDI, and surface charge of both empty (without the extract) and extract-loaded vesicles were assessed. Empty liposomes, nutriosomes, and alginate-nutriosomes were significantly smaller than their extract-loaded counterparts ($p<0.05$), suggesting the effective intercalation of phytocomplex components into the bilayer, which modified assembly and resulted in larger vesicles with reduced curvature radius. Empty liposomes were characterized by a small size of roughly 41 nm, a PDI near 0.33, and a negative charge of about −38 mV. The addition of Nutriose® or a combination of Nutriose® and alginate, substantially modifies the characteristics of the vesicles, which become larger (59 and 89 nm, respectively) and more negatively charged, especially alginate-nutriosomes (Table 2).

As previously documented in literature, incorporating an extract into vesicles can lead to a notable alteration in size, either increasing or decreasing, as a result of changes in the packing of phospholipids. This alteration may subsequently influence the assembly of the vesicles [6,17,49,50]. The incorporation of FEAE into the vesicles resulted in a significant increase in

the average diameter of liposomes, reaching approximately 105 nm, and nutriosomes, which expanded to around 124 nm. The presence of alginate slightly reduced vesicle enlargement in nutriosome (~115 nm) formulations. This effect is likely attributed to electrostatic interactions between the polymer and the phospholipid, which alter the assembly of the vesicles.

Furthermore, the addition of the FEAE significantly reduced the polydispersity indexes (PDI ≤ 0.19), indicating a more homogeneous size distribution (Table 2). The PDI is of immense importance in the homogeneity and stability of the particle size distribution [51]. A higher PDI value is observed in samples that encompass a more diverse array of sizes, in contrast to samples composed of uniformly sized particles, indicating that the PDI value reflects the distribution of particle sizes [52].

Besides, all the formulations exhibited a significantly negative zeta potential (from −32 to −56 mV), attributed to the presence of negatively charged phosphatidylcholine groups [53]. By increasing the electrostatic repulsion among vesicles, this approach could enhance the long-term storage stability in dispersion, thereby reducing the likelihood of agglomeration and fusion [54].

Table 2. Vesicle characterization: Mean diameter (MD), polydispersity index (PDI), zeta potential (ZP), Entrapment efficiency (EE), and Antioxidant activity. Mean values ± standard deviations are presented (n ≥ 6).

	MD (nm)	PDI (PDI)	ZP (mV)	EE (%)	AA (%)
Plain liposomes	41 ± 3	0.33	-38 ± 9	-	-
Plain nutriosomes	59 ± 4	0.29	-34 ± 2	-	-
Plain	89 ± 1	0.29	-57 ± 3	-	-

alginate-nutriosomes					
Liposomes	105 ± 3	0.18	-36 ± 3	97 ± 33	74 ± 65
Nutriosomes	124 ± 8	0.19	-32 ± 1	94 ± 24	72 ± 44
Alginate-nutriosomes	115 ± 8	0.18	-56 ± 8	98 ± 38	84 ± 41

3.3. Entrapment Efficiency

The entrapment efficiencies of all vesicles, irrespective of their composition, exceeded 90%, confirming the high capacity of these vesicular systems to retain high amount of active molecules, including highly hydrophilic phenolic compounds, with alginate-nutriosome nanoparticles showing the highest entrapment efficiency (98%). In nutriosomes, the binding process generally begins at the surface of the dextrin-rich fibers and subsequently proceeds through diffusion into the internal fiber matrix. This mechanism promotes interactions between the polyphenols present in the extract and the Nutriose® dextrin solubilized within the vesicular aqueous domains [17]. The incorporation of alginate further enhanced the loading capacity of the system. This improvement is likely attributable to the presence of anionic carboxyl groups, which can establish electrostatic interactions with the positively polarized regions of phospholipid headgroups, as well as hydrogen bonds with both phospholipids and polyphenols. These additional non-covalent interactions strengthen the overall structural cohesion of the vesicles, contributing to a more efficient and stable bilayer capable of protecting and retaining the encapsulated compounds throughout their biological journey [55]. These results highlight the strong impact of formulation composition on both the entrapment efficiency and the DPPH radical-scavenging activity of the FEAE-loaded vesicles. Our findings are fully consistent with previous research. For example, Flamminii et al. (2020) reported that the entrapment efficiency of phenolic extracts was markedly enhanced when using alginate–

casein or alginate–whey protein systems, an effect attributed to the strong intermolecular interactions provided by these polymers [56].

3.4. DPPH radical scavenging activity

As can be seen in Table 2, the DPPH radical scavenging activity of the FEAE-loaded vesicles varied between 72% and 84%, with the nutriosomes, liposomes, and alginate-nutriosome exhibiting activities of 72 %, 74 %, and 84 %, respectively. Considering the measured DPPH radical scavenging activity of the FEAE (88%), these outcomes indicate that loading the FEAE in the vesicles did not lead to a significant change in its antioxidant activity.

3.4. Stability of vesicles in simulated gastro-intestinal conditions

Oral administration is often the preferred method for delivering various drugs, as it is convenient, affordable, and secure, leading to improved adherence by patients [57]. Upon oral intake, formulations are mixed with media that possess different pH levels and ionic strengths throughout the gastrointestinal tract. Such conditions may lead to the breakdown of carriers and payloads, thereby compromising the efficacy of oral delivery [58]. Therefore, the vesicles were subjected to dilution and incubated at 37°C with an appropriate medium that simulates conditions typically encountered in the oral pathway.

The stability of FEAE-loaded vesicles was assessed in simulated salivary, gastric, and intestinal fluids. Vesicle size and PDI remained largely stable after 10 min incubation in salivary conditions (pH 6.75), with minor size increases (16–21 nm). In gastric conditions (pH 1.2, 2 h), vesicles exhibited larger diameter, particularly liposomes (+56 nm), nutriosomes (+62 nm), and alginate-nutriosomes (+40 nm), alongside increases in PDI. However, alginate-nutriosomes maintained superior structural integrity and lower PDIs compared to the other formulations. Similar trends were observed under intestinal conditions (pH 7.0, 6 h), where alginate-nutriosomes again

demonstrated the most stable behavior (Table 3). The combination of alginate with phospholipid based vesicles probably reinforced the membrane structure by establishing stronger non-covalent interactions, such as hydrogen bonding and electrostatic attractions between alginate's anionic carboxyl groups and the polar heads of phospholipids and polyphenols. Moreover, alginate could effectively interact with other polysaccharides through electrostatic interactions [59]. This internal polymeric network reduces membrane fluidity and enhances vesicle cohesiveness, thereby resisting destabilization caused by the pH variations of the gastrointestinal tract. Consequently, this leads to enhanced vesicle integrity and preserves vesicle size and homogeneity under harsh gastro-intestinal conditions, which are essential for the effective oral delivery and bioavailability of encapsulated compounds. Overall, this association seems to be ideal for achieving greater resistance, especially under acidic conditions.

Table 3. Mean diameter (MD), polydispersity index (PDI), and zeta potential (ZP) of the nanocarrier formulations diluted and incubated at 37 °C for 10 min at pH 6.75; 2 h at pH 1.2; or 6 h at pH 7.0. Mean values ± standard deviations are reported (n =3).

	pH	Time(min)	MD(nm)	PDI	ZP(mV)
Liposomes	6.75	10	126 ± 5	0.21	-18 ± 3
	1.20	120	161 ± 7	0.37	+ 4 ± 7
	7.00	360	139 ± 8	0.32	- 5 ± 4
Nutriosomes	6.75	10	142 ± 7	0.23	-22 ± 8
	1.20	120	186 ± 1	0.36	+8 ± 5
	7.00	360	151 ± 8	0.26	- 10 ± 1
Alginate-nutriosomes	6.75	10	131 ± 2	0.20	-26 ± 4
	1.20	120	155 ± 5	0.24	+ 4 ± 2
	7.00	360	125 ± 4	0.21	- 13 ± 5

3.5. FT-IR analysis

The FTIR spectra displayed in Figure 3 provide valuable insights into the structural characteristics of the polyphenol-rich FEAE and its molecular interactions when incorporated within phospholipid vesicular systems (Liposomes, nutriosomes, and algitate-nutriosomes).

All spectra represent broad absorption bands around 3200–3600 cm^{-1}, attributed to O–H stretching vibrations from hydroxyl groups. This band appears more intense and broader in the FEAE-loaded vesicles, indicating stronger hydrogen bonding interactions. These interactions probably occur between the hydroxyl groups of the polyphenolic compounds, and the functional groups present in the gum matrix or phospholipid bilayer, which contribute to structural stability [60,61]. The spectral region ranging from 1600 to 1700 cm^{-1}, which is generally linked to C=O stretching vibrations of carbonyl groups, does not exhibit any significant or clearly defined peaks across the various formulations. This observation implies a limited occurrence of free carbonyl-containing groups or potentially robust hydrogen bonding interactions that mask the carbonyl signals. The lack of notable peaks in this spectral range further supports the hypothesis that polyphenols are engaging with the carrier matrix instead of existing in a free state [62]. In the around 1000 cm^{-1} region, all samples showed characteristic peaks related to C–O–C and P–O vibrations. However, slight shifts and changes in peak intensity were observed in the FEAE-loaded vesicles compared to the blanks, suggesting interactions between the polyphenols and the polysaccharide–lipid matrix [61]. The fingerprint region (600–1300 cm^{-1}), especially between 600 and 900 cm^{-1}, showed slight but consistent changes in band intensity and shape in the FEAE-loaded samples. These alterations are linked to interactions involving sugar ring vibrations and aromatic structures, confirming that the polyphenols are not merely physically trapped but are closely integrated with the carrier matrix. Besides, the alginate-nutriosomes further display the most pronounced changes across O–H, C=O,

and ~1000 cm^{-1} regions, reflecting stronger and more diverse interactions, including hydrogen bonding and possible electrostatic effects. Collectively, these spectral modifications confirm successful entrapment of the FEAE, with the alginate-nutriosomes offering enhanced stabilization and enhanced molecular compatibility within the vesicular system.

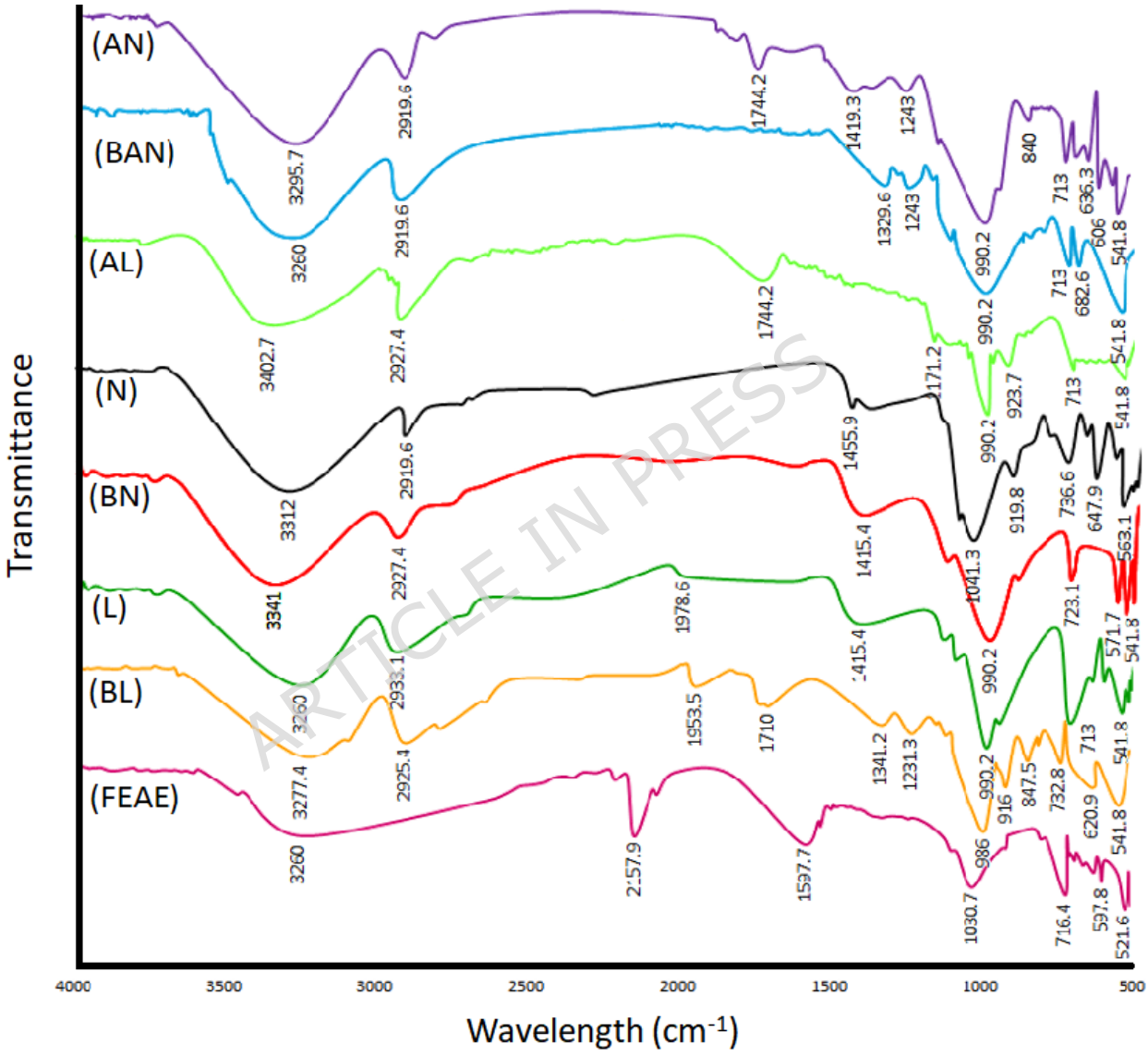

Figure 3. FT-IR spectra of FEAE, sodium alginate (AL), and the nanocarriers (BL: Blank liposome; L: Liposome; BN: Blank nutriosome; N: Nutriosome; BAN: Blank alginate-nutriosome; AN: Alginate-nutriosome).

3.6. In vitro release study

Figure 4 illustrates the release trend of the phytochemicals from all formulated vesicles over a 48 hours period at 37°C. Controlled release profiles were observed for all formulations. Cumulative release remained below 50% irrespective of the formulation tested, confirming sustained release properties. Alginate-nutriosomes showed the slowest release (~38%), followed by liposomes (~44%) and nutriosomes (~49%). As reported in Figure 4, the highest release occurred within the first 30 minutes, particularly in liposomes and nutriosomes (~24%), while alginate-nutriosomes exhibited significantly lower initial release (~14%). The observed release profile suggests that the extract is released primarily through a diffusion–controlled mechanism facilitated by the gradual swelling and partial erosion of the alginate matrix under intestinal pH conditions, providing insights into their potential effectiveness in delivering the compounds in vitro.

The sustained release profiles of all formulations further support their potential for controlled oral delivery. In particular, the delayed release profile of alginate-nutriosomes suggests the possibility of targeted intestinal delivery, minimizing early degradation of polyphenols in the upper gastro-intestinal tract and enhancing their bioaccessibility. Prior investigations have confirmed that alginates can be effectively employed as encapsulants and emulsifiers for the loading and delivery of diverse bioactive agents, including vitamins, minerals, essential fatty acids, peptides, essential oils, bioactive oils, polyphenols, and carotenoids. Moreover, the combination of alginate with other polysaccharides and emulsifiers has been acknowledged as the most effective and favorable approach for the protection, delivery, and sustained release of bioactive compounds [63].

The study by Norcino et al. (2022) indicated that alginate-pectin microcapsules provided better retention of anthocyanin and a more effective release profile during the process of intestinal digestion [64]. Furthermore,

findings from another study revealed that the combination of alginate-casein and alginate-whey protein enhanced the entrapment efficiency and the release of phenolic extracts during digestion, attributed to the robust interactions of these polymers [56]. These findings highlight the differences in release behavior among the formulations and underscore their effectiveness in modulating the release rate of the natural chemicals.

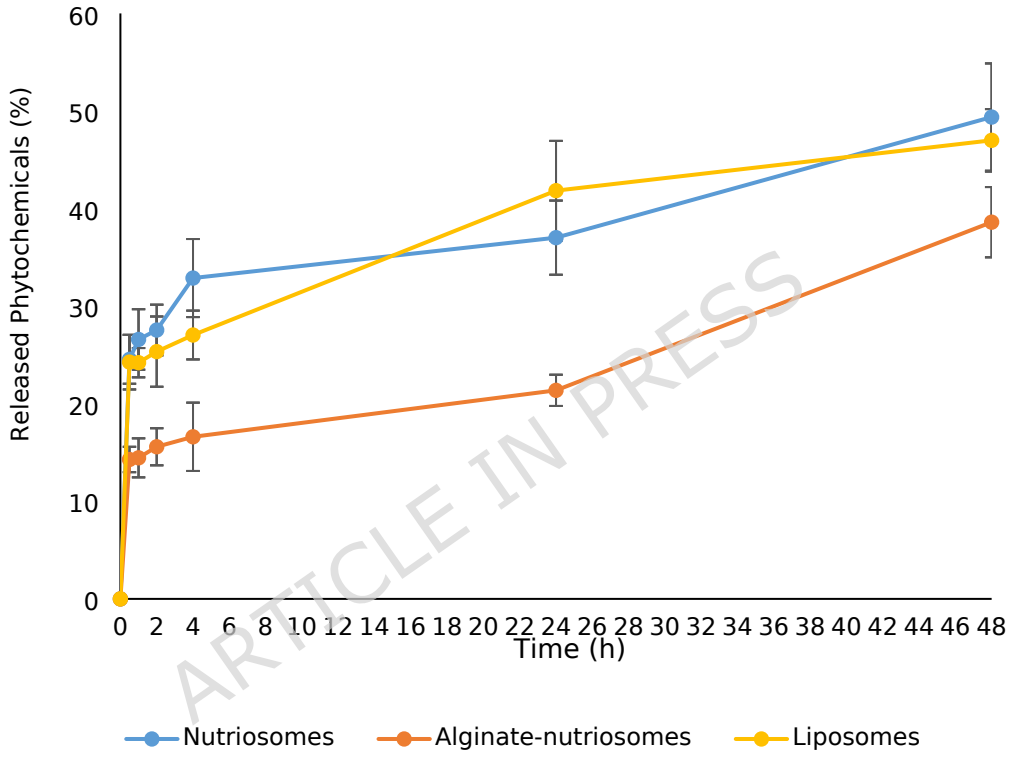

Figure 4. Amount of phytochemicals (%) released from liposomes, nutriosomes, and alginate-nutriosomes during 48 h of experiment at 37 °C. Mean values (error bars) ± standard deviations are reported (n = 3).

3.7. Biocompatibility and cytoprotective effect

An evaluation of the biocompatibility of FEAE, whether in dispersion or incorporated into the vesicles, was conducted using Caco-2 cells, representing a human colon-rectal epithelial model [65]. The cells were subjected to incubation for a duration of 48 h with samples at varying

dilutions, specifically 0.005, 0.05, 0.5, and 5 µg/mL of the extract. Prior research has established that this incubation period allows for a reliable cell viability assessment, whereas a longer 72-h exposure without medium replacement does not accurately reflect *in vivo* conditions [66]. Cell viability assays demonstrated that FEAE in aqueous dispersion is biocompatible, even if it slightly reduced Caco-2 cell viability to ~80%, independently of the concentration tested, while vesicle-loaded FEAE markedly improved cell viability. Notably, alginate-nutriosomes increased viability up to 130%, suggesting potential proliferative and/or protective effects (Figure 5A).

Importantly, biocompatibility assays revealed that vesicle entrapment not only preserved cell viability but, in the case of alginate-nutriosomes, appeared to promote cellular proliferation, possibly due to improved bioavailability and cellular uptake of phenolics. This is in line with previous studies reporting that nano-entrapment can modulate cellular responses and mitigate cytotoxicity often associated with high concentrations of free phenolic compounds [67]. Results on chitosan-sodium alginate-oleic acid nanocarrier for delivery of lutein revealed enhanced bioavailability and target delivery in a rat model with no toxicity [68]. Besides, guar gum-coated nano-nutriosomes containing cyanidin-3-*O*-glucoside showed increased cellular uptake without cytotoxicity [69]. Similarly, cyanidin-3-*O*-glucoside-loaded nano-nutriosomes, which are coated by Arabic gum, demonstrated biocompatibility and no cytotoxicity in Caco-2 cells [70].

A

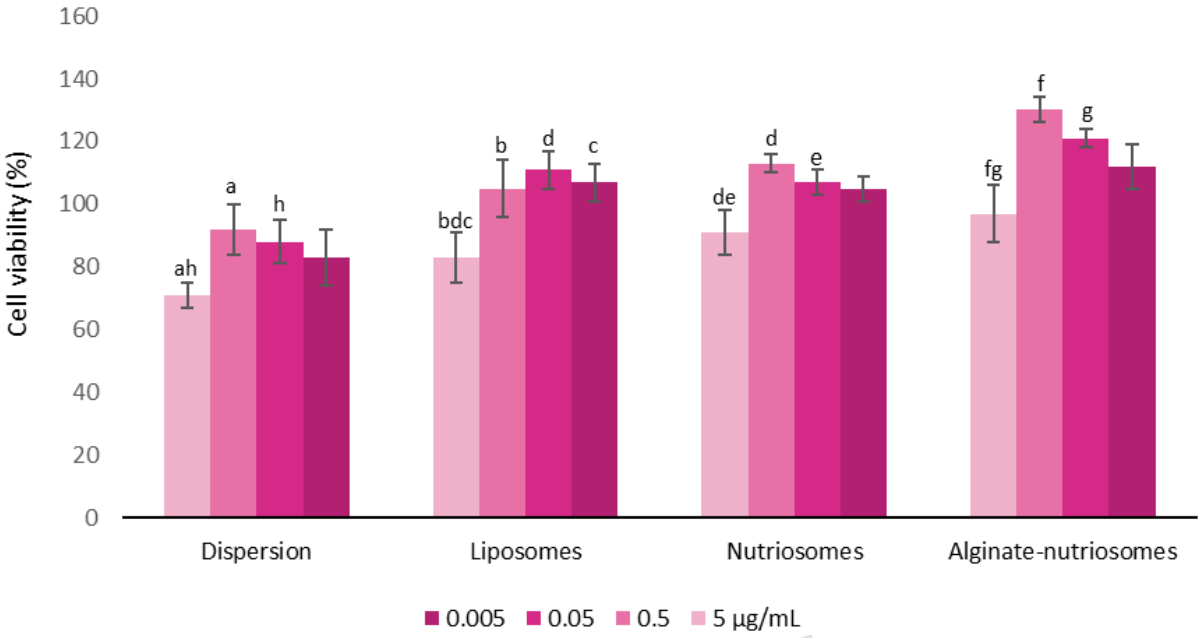

B

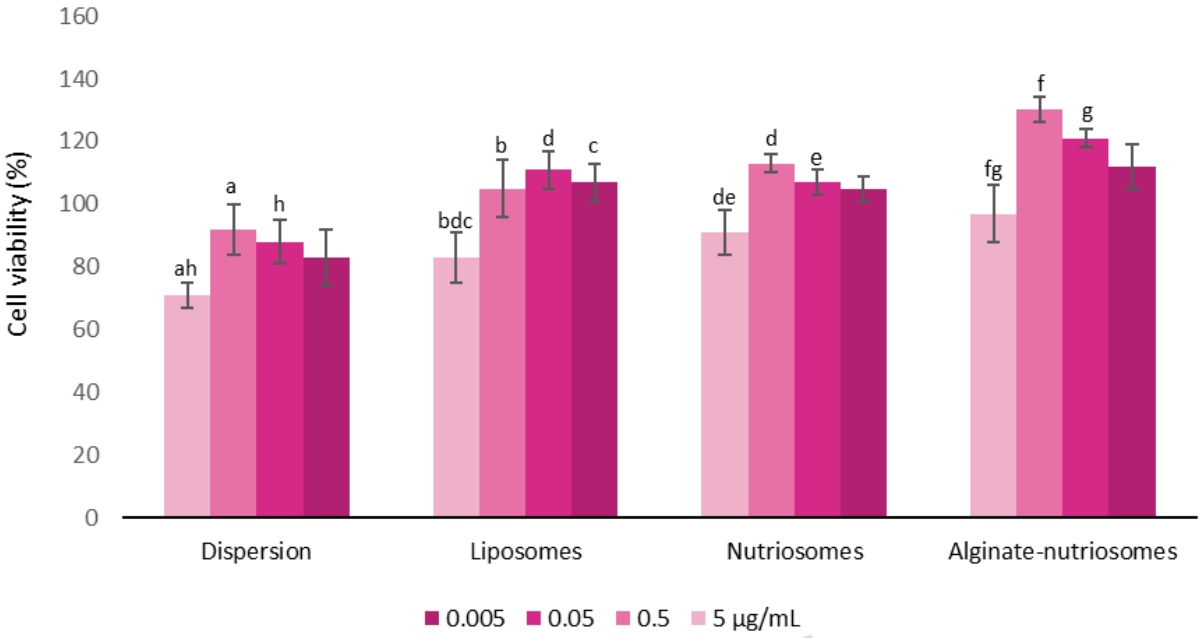

Figure 5. (A) Viability of Caco-2 cells incubated for 48 h with the FEAE in aqueous dispersion or loaded in liposomes, nutriosomes and alginate-nutriosomes..

(B) Viability of Caco-2 cells stressed with hydrogen peroxide and treated with FEAE in aqueous dispersion or loaded in vesicles. Mean values ± standard deviations are reported.

Mean values ± standard deviations are reported (n = 3). Different letters indicate values that are statistically different ($p < 0.05$)

The protective potential of extract-loaded vesicles against oxidative damage in intestinal cells was evaluated and compared to the efficacy of the extract in aqueous dispersion. Hydrogen peroxide (H_2O_2) serves as the most utilized inducer of cellular damage, mortality, and apoptosis in cells, in a manner that is dependent on both time and concentration. Upon exposure to oxidative stress (H_2O_2), untreated Caco-2 cells exhibited ~60% viability. FEAE in dispersion provided limited protection (~63.5%), while vesicle-loaded FEAE significantly improved protection, especially alginate-nutriosomes, which

maintained viability at ~94%, indicating superior and significant antioxidant protection at cellular level (Figure 5B).

The oxidative stress protection assay provides particularly encouraging data, showing that entrapment of FEAE into nanocarriers markedly improved the ability to counteract hydrogen peroxide-induced cytotoxicity in intestinal cells. These findings align with prior research, substantiating the safety and efficacy of the antioxidant extract-loaded phospholipid vesicles in protecting intestinal cells from oxidative stress-induced damage and death [6,17]. Alginate-nutriosomes conferred the highest level of protection, likely due to their superior entrapment efficiency, stability, and controlled release behavior, which together ensured a sustained antioxidant presence during the oxidative insult.

Overall, these findings highlight the synergistic effect of lactic acid fermentation and advanced vesicular entrapment in enhancing the stability, bioactivity, and therapeutic potential of plant-derived phenolics. In particular, alginate-nutriosomes emerge as highly promising nature-based delivery systems for future nutraceutical applications targeting gastro-intestinal health and oxidative stress-related disorders.

4. **Conclusion**

In this study, an innovative delivery system combining microbial fermentation using *L. plantarum* (DSM 20179) and advanced nanocarrier technology was successfully developed for the oral administration of polyphenol-rich *E. amoenum* extract. FEAE represented a high level of TPC and antioxidant activity, while the use of phospholipid-based vesicles, especially nutriosomes and alginate-nutriosomes, provided highly efficient entrapment, sustained release, and improved stability under gastro-intestinal conditions.

Among the developed formulations, alginate-nutriosomes demonstrated superior performance in terms of entrapment efficiency (98%), physical stability, controlled release profile, and protection against oxidative stress in Caco-2 cells. This enhanced biological activity highlights the synergistic effect of combining alginate, Nutriose, and phospholipids to improve the bioaccessibility and cellular efficacy of plant-derived polyphenols.

The preliminary but promising *in vitro* results suggest that alginate-nutriosomes may represent a safe, biocompatible, and effective oral delivery platform for natural chemicals, with potential applications in nutraceuticals, functional foods, and preventative healthcare strategies targeting oxidative stress and intestinal health.

Further *in vivo* investigations are warranted to validate the bioavailability, pharmacokinetics, and therapeutic benefits of these systems, and to explore their full potential in the clinical and commercial nutraceutical sectors.

Author Contributions

Ehsan Divan Khosroshahi: Conceptualization, Methodology, Investigation, Data curation, Formal analysis, Visualization, Writing – original draft, Writing – review and editing. Rita Abi Rached: Methodology, Investigation, Data curation, Formal analysis. Zeinab E. Mousavi: Validation, Writing – review and editing. Maryam Salami: Validation, Writing – review and editing. Angela Serpe: Data curation, Formal analysis. Mona Ghaslani: Data curation, Formal analysis. Maria Manconi: Conceptualization, Methodology, Data curation, Validation. Maria Letizia Manca: Supervision, Conceptualization, Methodology, Investigation, Data curation, Formal analysis, Visualization, Writing – original draft, Writing – review and editing. Osmolowskaya:

Validation, writing – review and editing. Seyed Hadi Razavi: Supervision, Conceptualization, Methodology, Investigation, Data curation, Formal analysis, Visualization, Writing – original draft, Writing – review and editing.

Funding

No funding for this review.

Declaration of competing interest

The authors declare that they have no conflict of interest.

Data availability

The datasets used and/or analysed during the current study are available from the corresponding author on reasonable request.

Acknowledgments

The authors would like to thank the Bioprocess Engineering Laboratory (BPEL), Department of Food Science and Engineering, Faculty of Agricultural Engineering and Technology, University of Tehran.

This publication has been produced with the financial assistance of: National Recovery and Resilience Plan (NRRP), Mission 4 Component 2 Investment 1.5-Call for tender No. 3277 published on 30 December 2021, by the Italian Ministry of University and Research (MUR) funded by the European Union—NextGenerationEU, Project Code ECS0000038-Project Title e. INS Ecosystem of Innovation for Next Generation Sardinia-Grant Assignment Decree No. 1056 adopted on 23 June 2022 and by the Italian Ministry of University and Research (MUR)

References

1. Sun, W. & Shahrajabian, M. H. Therapeutic Potential of Phenolic Compounds in Medicinal Plants—Natural Health Products for Human Health. *Molecules* **28**, 1845 (2023).

2. Divan Khosroshahi, E., Razavi, S. H., Salami, M. & Ubeyitogullari, A. Food Bioscience Recent advances in bioprocessing of medicinal plants through fermentation : A promising approach to maximize nutritional / functional value , bioactive potential , and health benefits. *Food Biosci* **70**, 107045 (2025).

3. Ivanova, S. *et al.* Medicinal plants: A source of phytobiotics for the feed additives. *J Agric Food Res* **16**, 101172 (2024).

4. Patel, K. & Patel, D. K. Potential medicinal application of phillygenin and atractylon in medicine as drug candidates with their molecular mechanism. *Food Biosci* **62**, 105075 (2024).

5. Berni, P. *et al.* The bioavailability of phytochemicals and its relation with health benefits on metabolic syndrome. *Improving Health and Nutrition through Bioactive Compounds* 125–147 (2025) doi:10.1016/B978-0-443-21873-6.00010-5.

6. Castangia, I. *et al.* From Grape By-Products to Enriched Yogurt Containing Pomace Extract Loaded in Nanotechnological Nutriosomes Tailored for Promoting Gastro-Intestinal Wellness. *Antioxidants* **12**, (2023).

7. Kumari, H. *et al.* Microbial transformation of some phytochemicals into value-added products: A review. *Fitoterapia* **178**, 106149 (2024).

8. Wu, X., Zhong, L., Chen, G., Zhong, S. & Gu, R. Morphological and physiological plasticity of alpine medicinal plants along an elevational gradient. *J Appl Res Med Aromat Plants* **44**, 100613 (2025).

9. Asghari, B. *et al.* Therapeutic target enzymes inhibitory potential, antioxidant activity, and rosmarinic acid content of Echium amoenum. *South African Journal of Botany* **120**, 191–197 (2019).

10. Firoznezhad, M. *et al.* Design and in vitro effectiveness evaluation of Echium amoenum extract loaded in bioadhesive phospholipid vesicles tailored for mucosal delivery. *Int J Pharm* **634**, (2023).

11. Darijani, S., Afsahi, M. M., Akhavan, H. R. & Goharrizi, A. S. Drying of borage (Echium amoenum) flowers extract: Optimization of encapsulation and spouted bed drying. *Applied Food Research* **5**, 100836 (2025).

12. Mehran, M., Masoum, S. & Memarzadeh, M. Improvement of thermal stability and antioxidant activity of anthocyanins of Echium amoenum petal using maltodextrin/modified starch combination as wall material. *Int J Biol Macromol* **148**, 768–776 (2020).

13. Khosroshahi, E. D. & Razavi, S. H. Wheat germ valorization by fermentation: A novel insight into the stabilization, nutritional/functional values and

therapeutic potentials with emphasis on anti-cancer effects. *Trends Food Sci Technol* **131**, 175–189 (2023).

14. Kucharska, E. *et al.* Potential Role of Bioactive Compounds: In Vitro Evaluation of the Antioxidant and Antimicrobial Activity of Fermented Milk Thistle. *Applied Sciences (Switzerland)* **14**, 1–22 (2024).

15. Hussain, A. *et al.* Fermentation, a feasible strategy for enhancing bioactivity of herbal medicines. *Food Research International* **81**, 1–16 (2016).

16. Khosroshahi, E. D., Razavi, S. H., Kaini, H. & Aghakhani, A. Improvement of stability and antioxidant activity of wheat germ by mixed fermentation versus single fermentation. *J Food Sci Technol* In press (2021) doi:10.1007/s13197-021-05316-w.

17. Perra, M. *et al.* A green and cost-effective approach for the efficient conversion of grape byproducts into innovative delivery systems tailored to ensure intestinal protection and gut microbiota fortification. *Innovative Food Science and Emerging Technologies* **80**, (2022).

18. Fulgheri, F. *et al.* Curcumin or quercetin loaded nutriosomes as oral adjuvants for malaria infections. *Int J Pharm* **643**, (2023).

19. Parekh, P. *et al.* Characterization of Nasco grape pomace-loaded nutriosomes and their neuroprotective effects in the MPTP mouse model of Parkinson's disease. *Front Pharmacol* **13**, 1–15 (2022).

20. Catalán-Latorre, A. *et al.* Nutriosomes: Prebiotic delivery systems combining phospholipids, a soluble dextrin and curcumin to counteract intestinal oxidative stress and inflammation. *Nanoscale* **10**, 1957–1969 (2018).

21. Pasman, W., Wils, D., Saniez, M.-H. & Kardinaal, A. Long-term gastrointestinal tolerance of NUTRIOSE®FB in healthy men. *Eur J Clin Nutr* **60**, 1024–1034 (2006).

22. Manca, M. L. *et al.* From waste to health: sustainable exploitation of grape pomace seed extract to manufacture antioxidant, regenerative and prebiotic nanovesicles within circular economy. *Sci Rep* **10**, 14184 (2020).

23. Manconi, M. *et al.* Bridging biotechnology and nanomedicine to produce biogreen whey-nanovesicles for intestinal health promotion. *Int J Pharm* **633**, 122631 (2023).

24. Castangia, I. *et al.* From Grape By-Products to Enriched Yogurt Containing Pomace Extract Loaded in Nanotechnological Nutriosomes Tailored for Promoting Gastro-Intestinal Wellness. *Antioxidants* **12**, 1285 (2023).

25. Rezvani, M. *et al.* Co-loading of ascorbic acid and tocopherol in eudragit-nutriosomes to counteract intestinal oxidative stress. *Pharmaceutics* **11**, (2019).

26. Perra, M. *et al.* A green and cost-effective approach for the efficient conversion of grape byproducts into innovative delivery systems tailored to ensure intestinal protection and gut microbiota fortification. *Innovative Food Science & Emerging Technologies* **80**, 103103 (2022).

27. Taweechaipaisankul, A. *et al.* Alginate-based encapsulation of porcine placenta extract: Preparation, enteric sustained release, biological activities, and stability. *Food Hydrocolloids for Health* **7**, 100194 (2025).

28. Abourehab, M. A. S. *et al.* Alginate as a Promising Biopolymer in Drug Delivery and Wound Healing: A Review of the State-of-the-Art. *International journal of molecular sciences* **23**, (2022).

29. Bi, D. *et al.* Potential Food and Nutraceutical Applications of Alginate: A Review. *Marine Drugs* **20**, 564 (2022).

30. Bounegru, A. V., Dima, Ş. & Apetrei, C. Determination of antioxidant capacity of glutathione encapsulated in alginate microcapsules using spectrophotometric and electrochemical methods. *Colloids Surf A Physicochem Eng Asp* **705**, 135735 (2025).

31. Harlen, W. C., Prakash, S., Yuliani, S. & Bhandari, B. Encapsulation of gallic acid in alginate/lactoferrin composite hydrogels: Physical properties and gallic acid diffusion. *Food Hydrocoll* **160**, 110784 (2025).

32. Khosroshahi, E. D., Razavi, S. H., Kiani, H. & Aghakhani, A. Mixed fermentation and electrospray drying for the development of a novel stabilized wheat germ powder containing highly viable probiotic cultures. *Food Sci Nutr* 1–10 (2023) doi:10.1002/fsn3.3092.

33. Khosroshahi, E. D., Razavi, S. H., Kaini, H. & Aghakhani, A. Improvement of stability and antioxidant activity of wheat germ by mixed fermentation versus single fermentation. *J Food Sci Technol* https://doi.org/10.1007/s13197-021-05316-w (2021) doi:10.1007/s13197-021-05316-w.

34. Castangia, I. *et al.* Phycocyanin-encapsulating hyalurosomes as carrier for skin delivery and protection from oxidative stress damage. *J Mater Sci Mater Med* **27**, 1–10 (2016).

35. Allaw, M. *et al.* Extraction, characterization and incorporation of hypericum scruglii extract in ad hoc formulated phospholipid vesicles designed for the treatment of skin diseases connected with oxidative stress. *Pharmaceutics* **12**, 1–20 (2020).

36. Manca, M. L. *et al.* Protective effect of grape extract phospholipid vesicles against oxidative stress skin damages. *Ind Crops Prod* **83**, 561–567 (2016).

37. Manca, M. L. *et al.* Molecular arrangements and interconnected bilayer formation induced by alcohol or polyalcohol in phospholipid vesicles. *Colloids Surf B Biointerfaces* **117**, 360–367 (2014).

38. Khosroshahi, E. D., Razavi, S. H., Kiani, H. & Aghakhani, A. Mixed fermentation and electrospray drying for the development of a novel stabilized wheat germ powder containing highly viable probiotic cultures. *Food Science and Nutrition* 1–10 (2023) doi:10.1002/fsn3.3092.

39. Khosravi, A., Razavi, S. H., Castangia, I. & Manca, M. L. Valorization of Date By-Products: Enhancement of Antioxidant and Antimicrobial Potentials through Fermentation. *Antioxidants* **13**, (2024).

40. Wang, L. *et al.* Role of carbohydrate-cleaving enzymes in phenolic mobilization of guava leaves tea during solid state bio-processing with Monascus anka and Bacillus sp. *Process Biochemistry* **82**, 51–58 (2019).

41. Akpoghelie, P. O. *et al.* Lactic acid bacteria: Nature, characterization, mode of action, products and applications. *Process Biochemistry* **152**, 1–28 (2025).

42. Tang, X. *et al.* Enhancing antioxidant activity of corn bract and silk juices through biotransformation of polyphenols by Lactobacillus paracasei TJ199 fermentation. *Food Chemistry: X* **28**, 102586 (2025).

43. Wang, T. *et al.* Metabolomics analysis reveals the effect of fermentation on the chemical composition and antioxidant activity of Paeonia lactiflora Root. *Heliyon* **10**, e28450 (2024).

44. Agatonovic-Kustrin, S., Gegechkori, V., Kustrin, E. & Morton, D. W. The effect of lactic acid fermentation on the phytochemical content of fig leaf extracts compared to single solvent and sequential solvents extraction. *South African Journal of Botany* **166**, 218–225 (2024).

45. Fessard, A. *et al.* Lactic Fermentation as an Efficient Tool to Enhance the Antioxidant Activity of Tropical Fruit Juices and Teas. *Microorganisms 2017, Vol. 5, Page 23* **5**, 23 (2017).

46. Eweys, A. S., Zhao, Y. S. & Darwesh, O. M. Improving the antioxidant and anticancer potential of Cinnamomum cassia via fermentation with Lactobacillus plantarum. *Biotechnology Reports* **36**, e00768 (2022).

47. Zhang, Q. *et al.* Effects of single and co-cultured lactic acid bacteria on antioxidant capacity and metabolite profiles during rambutan juice fermentation. *Food Chemistry: X* **30**, 102904 (2025).

48. Tan, Y. *et al.* Functional components and antioxidant activity were improved in ginger fermented by Bifidobacterium adolescentis and Monascus purpureus. *Lwt* **197**, 1–9 (2024).

49. Kurbonova, M. *et al.* Chitosan-coated liposomes of pomegranate-peel phenolic extract: Maximizing the bioaccessibility and antimicrobial activity in probiotic goat yoghurt. *J Stored Prod Res* **112**, 102600 (2025).

50. Bonechi, C. *et al.* Cationic liposomes as carriers of natural compounds from plant extract. *Biophys Chem* **318**, 107381 (2025).

51. Ledri, S. A., Milani, J. M., Shahidi, S. A. & Golkar, A. Comparative analysis of freeze drying and spray drying methods for encapsulation of chlorophyll with maltodextrin and whey protein isolate. *Food Chem X* **21**, 101156 (2024).

52. Ahmadian, S., Kenari, R. E., Amiri, Z. R., Sohbatzadeh, F. & Khodaparast, M. H. H. Fabrication of double nano-emulsions loaded with hyssop (Hyssopus officinalis L.) extract stabilized with soy protein isolate alone and combined with chia seed gum in controlling the oxidative stability of canola oil. *Food Chem* **430**, 137093 (2024).

53. Zhou, Y. & Raphael, R. M. Solution pH Alters Mechanical and Electrical Properties of Phosphatidylcholine Membranes: Relation between Interfacial Electrostatics, Intramembrane Potential, and Bending Elasticity. *Biophys J* **92**, 2451–2462 (2007).

54. Gilbile, D. *et al.* How Well Can You Tailor the Charge of Lipid Vesicles? *Langmuir* **35**, 15960–15969 (2019).

55. Kadri, R. *et al.* Role of active nanoliposomes in the surface and bulk mechanical properties of hybrid hydrogels. *Materials Today Bio* **6**, 100046 (2020).

56. Flamminii, F. *et al.* Structuring alginate beads with different biopolymers for the development of functional ingredients loaded with olive leaves phenolic extract. *Food Hydrocoll* **108**, 105849 (2020).

57. Günday Türeli, N. & Türeli, A. E. Industrial perspectives and future of oral drug delivery. *Nanotechnology for Oral Drug Delivery: From Concept to Applications* 483–502 (2020) doi:10.1016/B978-0-12-818038-9.00016-8.

58. Costa, J. R. *et al.* Impact of in vitro gastrointestinal digestion on the chemical composition, bioactive properties, and cytotoxicity of Vitis vinifera L. cv. Syrah grape pomace extract. *Food Funct* **10**, 1856–1869 (2019).

59. Xie, F., Gao, C. & Avérous, L. Alginate-based materials: Enhancing properties through multiphase formulation design and processing innovation. *Materials Science and Engineering: R: Reports* **159**, 100799 (2024).

60. Mahdavi, S. A., Jafari, S. M., Ghorbani, M. & Assadpoor, E. Spray-Drying Microencapsulation of Anthocyanins by Natural Biopolymers: A Review. *Drying Technology* **32**, 509–518 (2014).

61. Liang, J., Li, H., Han, M. & Gao, Z. Polysaccharide-polyphenol interactions: a comprehensive review from food processing to digestion and metabolism. *Critical Reviews in Food Science and Nutrition* **65**, 3459–3475 (2025).

62. Liu, X., Le Bourvellec, C. & Renard, C. M. G. C. Interactions between cell wall polysaccharides and polyphenols: Effect of molecular internal structure. *Comprehensive Reviews in Food Science and Food Safety* **19**, 3574–3617 (2020).

63. Karim, A. *et al.* Alginate-based nanocarriers for the delivery and controlled-release of bioactive compounds. *Advances in Colloid and Interface Science* **307**, (2022).

64. Norcino, L. B. *et al.* Development of alginate/pectin microcapsules by a dual process combining emulsification and ultrasonic gelation for encapsulation and controlled release of anthocyanins from grapes (Vitis labrusca L.). *Food Chem* **391**, 133256 (2022).

65. Verhoeckx, K. *et al.* The impact of food bioactives on health: In vitro and Ex Vivo models. *The Impact of Food Bioactives on Health: In Vitro and Ex Vivo Models* 1–327 (2015) doi:10.1007/978-3-319-16104-4,.

66. Castangia, I. *et al.* Mouthwash Formulation Co-Delivering Quercetin and Mint Oil in Liposomes Improved with Glycol and Ethanol and Tailored for Protecting and Tackling Oral Cavity. *Antioxidants 2022, Vol. 11, Page 367* **11**, 367 (2022).

67. Garavand, F., Jalai-Jivan, M., Assadpour, E. & Jafari, S. M. Encapsulation of phenolic compounds within nano/microemulsion systems: A review. *Food Chem* **364**, 130376 (2021).

68. Toragall, V., Jayapala, N., S P, M. & Vallikanan, B. Biodegradable chitosan-sodium alginate-oleic acid nanocarrier promotes bioavailability and target delivery of lutein in rat model with no toxicity. *Food Chemistry* **330**, 127195 (2020).

69. Paul, B. *et al.* Development and evaluation of guar gum-coated nano-nutriosomes for cyanidin-3-O-glucoside encapsulation. *International Journal of Biological Macromolecules* **271**, 132537 (2024).

70. Xie, L. *et al.* Green synthesis, characterization, food simulants stability, and antioxidant activity of gum Arabic-coated cyanidin-3-O-glucoside-loaded nano-nutriosomes. *Food Hydrocolloids* **154**, 110083 (2024).